平 成 ２ ７ 年 度

京 都 大 学 大 学 院 理 学 研 究 科

ＤＣ３回生研究発表会
要旨集

２０１５年１１月２４日（火）

物 理 学 第 一 分 野

物理学第一分野ＤＣ３回生研究発表会

場所：理学研究科５号館　５階・第四講義室
発表：１５分（別に質問１０分程度）

２０１５年１１月２４日（火）９：００～　開始

目　　次

１５：１０～１５：２０　休憩

１７：００～１７：１０　休憩

Derivation of Stokes' law without the hydrodynamic equations

Nonlinear Dynamics Group Masato Itami

Abstract We study the friction coefficient of a macroscopic sphere in a viscous fluid at low Reynolds number. By combining Kirkwood's formula and the Green–Kubo formula in large deviation theory, we derive Stokes' law without explicitly employing the hydrodynamic equations.

In equilibrium systems, macroscopic behavior is systematically described by a universal framework—thermodynamics. On the basis of a microscopic description of equilibrium systems, the principle of equal a priori probabilities and Boltzmann's principle reproduce the framework of thermodynamics, which is established as equilibrium statistical mechanics. In contrast, there is still no theory describing the general behavior of non-equilibrium systems beyond the linear response regime. Thus, much effort has been devoted to the investigation of steady-state thermodynamics and non-equilibrium statistical mechanics.

When liquids and gases are out of equilibrium but still remain in local equilibrium, their macroscopic dynamical behavior is precisely described by the hydrodynamic equations. A microscopic understanding of the hydrodynamic equations for the case of dilute gases was established through the Boltzmann equation, whereas it remains unclear for a general fluid. Non-trivial relations that are generally valid far from equilibrium, including the fluctuation theorems and the Jarzynski equality, have been developed over the past two decades as a result of the time-reversal symmetry of microscopic mechanics. Thanks to such universal relations, we can easily re-derive certain well-known relations, such as the McLennan ensembles, the Green–Kubo formula, and the Kawasaki nonlinear response relation. Furthermore, by using a non-equilibrium identity similar to the fluctuation theorems and assuming a local Gibbs distribution at the initial time, the Navier–Stokes equation was derived for an isolated Hamiltonian system [1]. Based on these achievements, we believe this is an opportune moment to reconsider fluid dynamics from the viewpoint of statistical mechanics.

In this presentation, we study the friction coefficient of a macroscopic sphere in a viscous fluid at low Reynolds number from the viewpoint of statistical mechanics. First, according to Kirkwood's formula [2], the friction coefficient is expressed in terms of the stress correlation on the surface of the macroscopic sphere. The stress correlation in the bulk of the fluid is characterized by the viscosity in the Green–Kubo formula [3]. Then, we establish the connection between the bulk and surface stress fluctuations. The basic concept is simple. The probability density of surface stress fluctuations is obtained from the probability density of bulk stress fluctuations by integrating out the other degrees of freedom. This procedure can be conducted in an elegant manner with the aid of large deviation theory. Finally, by combining Kirkwood's formula and the Green–Kubo formula in large deviation theory, we derive Stokes' law [4] without explicitly employing the hydrodynamic equations [5].

References

[1] S. Sasa, Phys. Rev. Lett. **112**, 100602 (2014).
[2] J. Kirkwood, J. Chem. Phys. **14**, 180-201 (1946).
[3] M.S. Green, J. Chem. Phys. **22**, 398-413 (1954).
[4] G.G. Stokes, Trans. Cambridge Philos. Soc. **9**, 8-106 (1851).
[5] M. Itami and S. Sasa, J. Stat. Phys. **161**, 532-552 (2015).

Shape fluctuation and deformation of biological soft interfaces

Dissipative structure and Biological physics laboratory　Hiroaki Ito

Abstract To understand the complex behaviors of cell membranes as non-equilibrium interfacial phenomena, we experimentally investigated the shape fluctuation and deformation of biological soft interfaces, consisting of lipid membrane and underlying cytoskeletal structure, using living and non-living systems, especially through the aspect of the interplay between them.

Cell membrane is a soft interface consisting of a phospholipid fluid bilayer in which large amount of membrane proteins are embedded. The membrane is further connected to underlying cytoskeletal network structure, and carries out a number of biological processes under the fluctuation and flexible deformation. In our recent works, we have experimentally investigated the characteristic interfacial phenomena of biological matters to understand the fundamental properties of cell membrane fluctuation and deformation. For example, we focused on the shape fluctuation of a red blood cell as the simplest membrane/cytoskeleton system. By combining a microfluidic technique and the wavenumber analysis of the shape fluctuation, called flicker spectroscopy, we directly compared the fluctuations before and after the influence of toxic agent, lipopolysaccharides, and confirmed the clear increasing effect on the attractive interaction between the cell membrane and cytoskeleton[1].

In contrast to the above passive fluctuation, in living organisms, active membrane deformation plays crucial roles in various biological processes, such as cell motility, cell division, embryonic development, etc. These dynamic membrane deformations are mainly caused by the active force generation by actomyosin, which is a protein complex of actin filaments and type II myosin. For the better understanding of the native properties of actomyosin, bottom-up/reconstituted systems have been adopted using only a small number of components involved in the force generation so far[2]. These studies have successfully verified the active contractile property of purified actomyosin and its higher order structure formation. To reveal the fundamental contribution of this active force generation to a deformable soft interface, we have developed a reconstituted experimental system, namely cell-sized water-in-oil droplets with lipid layers connected to actin and myosin by electrostatic attraction. As a result, we successfully reconstituted the active membrane fluctuation and deformation driven by actomyosin *in vitro* for the first time; we observed (i) non-periodic oscillatory undulation and (ii) curvature-dependent dynamic deformation of the interface induced by the contractile force of actomyosin hierarchical structures (Fig.1)[3].

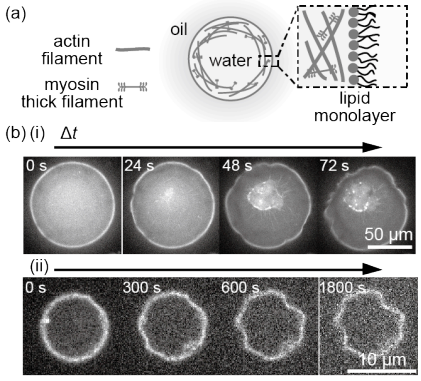

Fig. 1. (a) Reconstituted system. (b) (i) active fluctuation and (ii) dynamic deformation induced by actomyosin in a reconstituted system.

References

[1] H. Ito *et al.*, J. Phys. Chem. B **119**, 7837-7845 (2015).
[2] K. Takiguchi *et al.*, Langmuir **27**, 11528-11535 (2011).; K. Carvalho *et al.*, PNAS **110**, 16456-16461 (2013).
[3] H. Ito *et al.*, arXiv:1505.04371v2 (2015).

Nonlinear analysis of the interfacial layer effects on the surface capacitances and electro-osmosis in electrolyte solutions

Phase Transition Dynamics Group Yuki Uematsu

Abstract We investigate the structure of electric double layer with effects of Stern layer. We construct an approximation for a modified Gouy-Chapman model with inhomogeneous dielectric constant and viscosity. Nonlinear analysis reproduces the numerical solution of the original equation. Also, the surface capacitance and the electro-osmotic mobility are calculated.

Electro-osmosis is the motion of electrolyte solutions induced by electric field across a capillary tube. It plays important roles in many systems such as industry and bio-systems. A well-known model describing the electro-osmosis is based on Poisson-Boltzmann and hydrodynamic equations. They describe electric diffuse double layers near a charged flat surface. However, this model cannot reproduce some experimental observations such as the surface capacitances and the saturation of electrokinetic surface charge correctly. Then a modified Poisson-Boltzmann equation considering the interfacial (Stern) layer effect was proposed [1]. It is given by

$$\frac{d^2\Psi}{dz^2} = \begin{cases} \varepsilon\kappa^2 \sinh\Psi & \text{for } 0 < z < z^* \\ \kappa^2 \sinh\Psi & \text{for } z^* < z \end{cases} \tag{1}$$

where $\Psi = e\psi / k_{\mathrm{B}}T$ is the dimensionless electrostatic potential, z^* = 0.1 nm is the thickness of the interfacial layer, ε =80.4 is the dielectric constant of water, and κ^{-1} is the Debye length. The temperature T is set to 300 K. However, eq. (1) is still difficult to solve analytically because its general solution contains elliptic functions. Then, we approximate eq. (1) by neglecting the existence of co-ion in the interfacial layer [2]. Assuming that the surface is negatively charged and the co-ion is cation, eq. (1) is rewritten to

$$\frac{d^2\Psi}{dz^2} = \begin{cases} -\dfrac{\varepsilon\kappa^2}{2}\mathrm{e}^{-\Psi} & \text{for } 0 < z < z^* \\ \kappa^2 \sinh\Psi & \text{for } z^* < z \end{cases} \tag{2}$$

This approximation is reasonable for the surface with $-\Psi << 1$ in the interfacial layer. We obtained the analytical solution of eq. (2) and discussed whether the approximation is valid or not by comparing the numerical results of eq. (1) and the analytical solution of eq. (2). Fig.1 shows the comparisons for various quantities. Clearly, this approximation works well when the surface potential is negative and the salt concentration is sufficiently low.

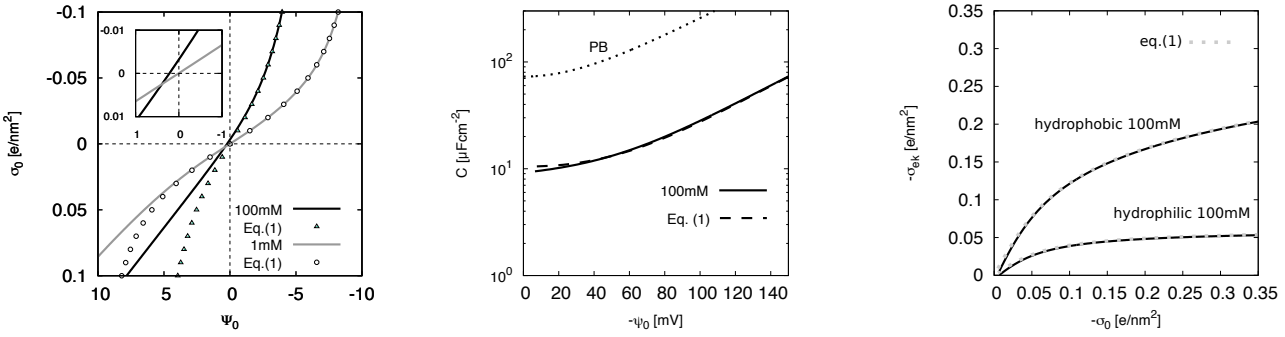

Fig. 1. (Left) Surface charge density as functions of the surface potential. (Center) Surface capacitance as functions of the surface potential. (Right) Electrokinetic surface charge density as functions of the bare surface charge density.

References

[1] D. J. Bonthuis and R. R. Netz, Langmuir **28**, 16049 (2012).

[2] Y. Uematsu, D. J. Bonthuis, and R. R. Netz, in preparation.

Disorder effects on quantum phase transition of ^{4}He in nanoporous media

Condensed matter theory group Yu Ogata

Abstract We theoretically investigate disorder effects on the quantum phase transition of ^{4}He in nanoporous media. We show that the randomness of media extends the superfluid region to low temperature and high pressure area, leading to the existence of the Bose glass phase at higher pressure.

Recently, ^{4}He confined in nanoporous media which has a 3D random network structure of a few nm pores has attracted much attention. The superfluid transition temperature T_c is drastically suppressed with increasing pressure and approaches 0 K at a critical pressure P_c [1]. Moreover, it is revealed that there exists a localized BEC (LBEC) state where BEC "islands" are grown in broader pores at higher temperatures and pressures than the superfluid phase boundary [2, 3]. The LBEC intervenes between the normal and the superfluid phases.

The suppression of T_c is theoretically explained by the Josephson junction array model with no randomness. However, the deviation from the experimental data still exists near the apparent quantum critical point (QCP). It would originate from the disorder effect.

In order to clarify the behavior near the QCP, we investigate disorder effects on the system. We introduce the randomness into the Josephson coupling term connecting between LBEC islands. The obtained phase diagram is shown in Fig. 1. First, the superfluid region is highly extended to low temperature and high pressure area. Second, the Bose glass phase, which is characteristic of the system with randomness, appears at higher pressure. We explain the deviation which has not been explained in a previous study [4], and propose the nature of quantum phase transition in this system.

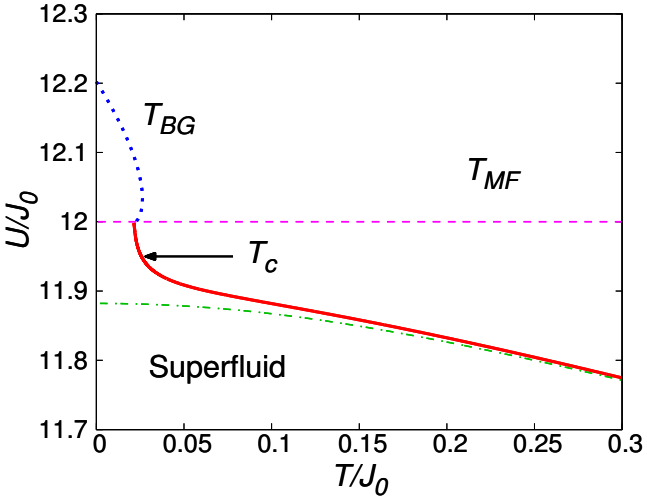

Fig. 1. Pressure-temperature phase diagram.

References

[1] K. Yamamoto, H. Nakashima, Y. Shibayama, and K. Shirahama, Phys. Rev. Lett. **93**, 075302 (2004).
[2] K. Yamamoto, Y. Shibayama, and K. Shirahama, Phys. Rev. Lett. **100**, 195301 (2008).
[3] J. Bossy, J. V. Pearce, H. Schober, and H. R. Glyde, Phys. Rev. B **78**, 224507 (2008).
[4] T. Eggel, M. Oshikawa, and K. Shirahama, Phys. Rev. B **84**, 020515(R) (2011).

Mode bifurcation of a chiral asymmetric dumbbell on a vertically vibrated plate

Dissipative structure and Biological physics laboratory　Yoshitsugu KUBO

Abstract We studied the behavior of a chiral asymmetric dumbbell bouncing upon a sinusoidally vibrating plate. We observed a cascade of bifurcations with an increase in the vibration amplitude: spinning, orbital, and rolling. The mode bifurcation from directional motion to random motion is interpreted analytically by a simple mechanics.

Spatiotemporal self-organization under nonequilibrium is one of intriguing research topics in modern physics. Sometimes a simple system involves rich nonlinear behaviors under nonequilibrium conditions. For example, just a bouncing object has attracted considerable interest, where various bifurcations, including the appearance of chaos, have been reported [1-3]. It has been shown that an axisymmetric dimer moves either forward or backward, depending on the initial conditions [1]. In this study, we demonstrate how the breaking of chiral symmetry creates a new scenario in the mode bifurcation of a bouncing dumbbell on a vibrating plate. Two-dimensional motions on the horizontally set plate, such as orbital and spin motions, were observed even though the plate was applied only vertical agitation isotopically.

In the experiment, cascade of different modes on two-dimensional motions were observed by introducing chiral asymmetry into a dumbbell particle under vertical vibration. By increasing vibration strength of the plate, spinning motion accompanied by random behavior of the centroid, now denoted SR mode, and spinning motion accompanied by directional motion (O mode) were emerged after translationally random motion. In addition, the SR and the O modes switched in a subcritical manner as a function of Γ, which is a normalized order parameter describing vibration strength. It was also shown that the angular velocity of the spinning motion that originates in the chirality is determined by sin(β'/2). A simple mechanical model was considered to obtain the lower limit of Γ for the directional motion of the dumbbell. Figure 1 shows that the estimated critical acceleration Γc agreed well with the experimental results and with simulation results which reproduces bifurcation between SR and O modes. The condition for periodic collision of the upper sphere appeared to have functional form identical to that of a single bouncing ball.

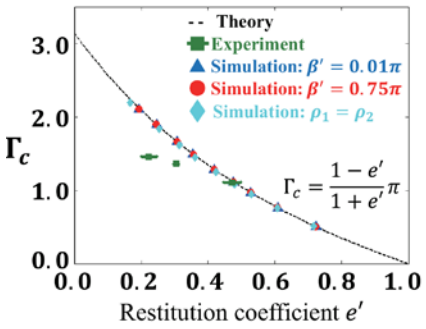

FIG..1. Dependence of the critical acceleration Γc on the restitution coefficient e.' Lower limit of steady collision in the theoretical analysis (dotted line), experiments (green square), and numerical simulation with β' = 0.01π (blue triangles), β' = 0.75π (red circles), and ρ1 = ρ2 (cyan diamonds). Experimental data are given for rubber (e' = 0.223 ± 0.024), aluminum (e' = 0.305 ± 0.008), and glass plates (e' = 0.472 ± 0.026).

.

[1] S. Dorbolo, D. Volfson, L. Tsimring, and A. Kudrolli, Dynamics of a Bouncing Dimer, Phys. Rev. Lett. 95, 044101 (2005).

[2] D. Yamada, T. Hondou, and M. Sano, Coherent dynamics of an asymmetric particle in a vertically vibrating bed, Phys. Rev. E 67, 040301 (2003).

[3] J. Wang, C. Liu, Y.-B. Jia, and D. Ma, Ratchet rotation of a 3D dimer on a vibrating plate, Eur. Phys. J. E 37, 1 (2014).

Coherence resonance occurred in oscillatory motion of a micrometer-sized droplet between electrode needles

Dissipative structure and Biological Physics Group　Tomo Kurimura

Abstract We have discovered the oscillating water droplet in an oil phase between the cone-shaped electrodes as a limit cycle. We found the noise can make the system oscillate when the voltage was slightly lower than the threshold. The result shows the new way to design an efficient nanometer-sized machine.

The small world is sticky and noisy. Viscosity is dominant in comparison with the inertia at the micrometer scale. Thermal fluctuation becomes significant in the motions of micro- to nano-objects. The conditions under which the micro- and nano-machines will be working require continuous force for continuous motion and resistibility against thermal noise. When we make such a machine in the conventional engineering way, it would be hard to reproduce the desired motion, as we are doing. For this reason, we have to find an innovative way to construct a nano- or micro-machine. One way to overcome this difficulty is to use or study the mechanism of biological motor proteins, which already exist in organisms [1]. The features of the mechanism will be utilized in the driving forces of the surrounding noisy environment. In our study, we used the micro-sized oscillation that is robust for perturbation, the limit cycle oscillation, and demonstrated that the system can generate a regular motion despite adding noisy external force.

At first, we briefly introduce a limit cycle oscillation. The difference of the limit cycle for a normal oscillation in a conservative system is a stable orbital. The track of the limit cycle is attractive and independent of the initial value. When one of the parameters substituting for an order parameter was increased or decreased, the system changed from oscillatory to stationary by crossing a bifurcation point. Below this threshold, the system would take an excitable state. In the excitable state, the system does not oscillate autonomously but shows asymptotic oscillation for one period stimulated by external force. Numerical simulations have shown that adding noisy external forces induces an excitable state of the pseudo limit cycle oscillation. This oscillatory behavior is called coherence resonance. We discovered an oscillation of a water droplet in an oil phase between cone-shaped electrodes and confirmed this oscillation as a limit cycle. Charging and discharging of the droplet at the electrodes, and electric and dielectric forces cause this cycle. We also observed that the system reaches an excitable state near the threshold voltage. We here tried to generate an oscillation on the system below the threshold by adding noisy external perturbation. Noise application successfully caused the system to oscillate even when the voltage is slightly lower than the threshold. The oscillation strength resonates with the magnitude of noise (Fig. 1).

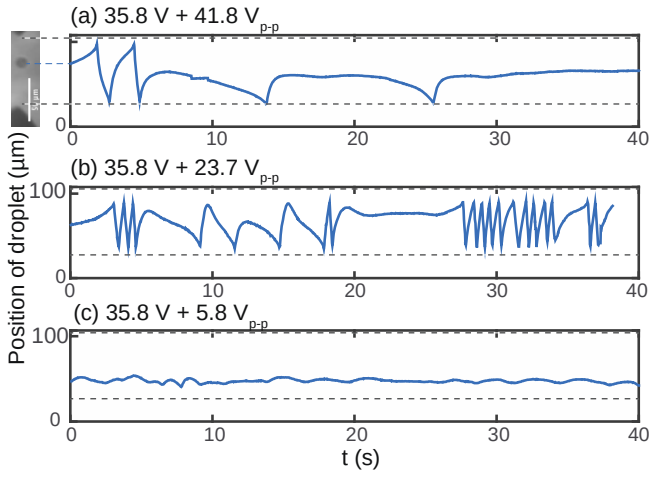

Fig. 1 Time Evolution of the droplet position. The voltage from the amplifier is (a) 35.8 V + 41.8 V_{p-p}, (b) 35.8 V + 23.7 V_{p-p}, (c) 35.8 V + 5.8 V_{p-p}. The position of the droplet was measured along the line between the electrodes. The position of electrodes is about 100 and 20 μ m (the dashed lines).

This phenomenon indicates a novel approach for nano-machines in which rhythmically ordered motion can be stabilized by the utilization of a noisy external force.

References

[1] M. G. L. van den Heuvel, Science, 317 333(2007)

An ultracold Fermi gas with localized impurities in an optical lattice with controllable interaction

Quantum Optics Group Hideki Konishi

Abstract Lifetimes of the metastable $^3P_2$ state of ytterbium (Yb) in the presence of the $^2S_{1/2}$ ground state of lithium (Li) in an optical lattice were measured. A fast decay due to inelastic collision between Yb and Li was observed. A search for Yb($^3P_2$)-Li($^2S_{1/2}$) Feshbach resonances is now underway.

Over the last two decades ultracold atoms have proven to be a valuable system to investigate quantum many-body physics. We can explore wide range of research fields thanks to useful tools such as optical lattices, defect-free periodic potential made by standing wave of light, and Feshbach resonances, controlling of interatomic interactions by magnetic field. Applying these techniques on an ultracold atomic mixture composed of a mass-imbalanced atomic pair, one can design a system of atoms subject to different dimensions [1].

An ultracold mixture of ytterbium (Yb) and lithium (Li), which has an extreme mass imbalance of about 29, is one of the promising systems to study physics in mixed dimensions. Loaded in an optical lattice, Yb atoms are deeply localized in lattice sites while Li atoms are itinerant over a whole system, which realizes a mixture of Yb atoms confined in low dimensions and a three-dimensional Li atomic gas. As for the inter-species interaction, unlike well-used alkali atom pairs, there are no usable Feshbach resonances between the ground states of Yb and Li. However, the metastable excited $^3P_2$ state of Yb offers an interesting possibility to tune interaction between Yb($^3P_2$) and Li by means of Feshbach resonances. In fact, Feshbach resonances between Yb in the $^3P_2$ state and Li in the ground state are discussed both in theory and experiment. [2, 3, 4].

As a first step, we developed a method to compensate gravitational sag between Yb and Li to obtain a spatial overlap of two atom clouds. Combining this method with an ultra-narrow optical transition of $^1S_0$-$^3P_2$ for impurity atoms of Yb, we could successfully observe the collisional instability of ^{174}Yb($^3P_2$) induced by Li($^2S_{1/2}$). A typical result at 3 Gauss is shown in Fig. 1. A faster decay was observed in the case with Li. The fast decay time constant was determined to be about 20 ms while the slow decay was about 1000 ms. Here we note that, by exciting singly-occupying Yb atoms in a Mott-insulator state in an optical lattice, the results get insensitive to unwanted Yb($^3P_2$)-Yb($^3P_2$) and Yb($^3P_2$)-Yb($^1S_0$) collisional channels. In this way, we could demonstrate the modification of the inelastic collision property between the Fermi gas of Li and the impurity atoms of Yb localized in an optical lattice.

To find usable ^{174}Yb($^3P_2$)-Li Feshbach resonances, we are now repeating the decay measurement of the ^{174}Yb($^3P_2$) in the presence of Li for various magnetic fields. Also we try fermionic ^{173}Yb that is expected to be more favorable to induce Feshbach resonances, because it has many hyperfine structures, which allow many channels to couple.

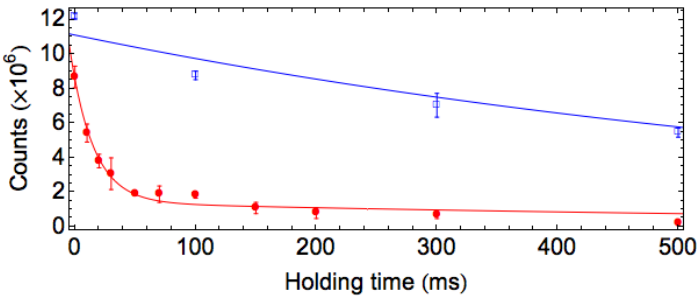

Fig. 1. Observed decay of the $^3P_2$ (m_J = 0) state of ^{174}Yb atoms in an optical lattice with Li (filled red circle) and without Li (open blue square) at 3.0 G of magnetic field. Lines are fits to the data.

References

[1] Y. Nishida, Phys. Rev. A **82**, 011605.
[2] A. Petrov *et al.*, New J. Phys. **17**, 045010 (2015).
[3] T. Chen *et al.*, New J. Phys. **17**, 103036 (2015).
[4] W. Dowd *et al.*, New J. Phys. **17**, 055007 (2015).

Emergent quantum phenomena in inhomogeneous optical lattices

Condensed matter theory group Masaru Sakaida

Abstract We investigate the attractively interacting Fermi systems with spatial nonuniformity. A statistical dynamical mean-field theory and a Bogoliubov-de Gennes method are extended to analyze the systems considered here. Employing these methods, we elucidate how disorder and interaction compete/cooperate with each other. Also, the disorder-triggered transitions in multicomponent systems are uncovered.

Thanks to high controllability, optical lattices with spatial nonuniformity have been successfully realized. One of the notable advantages of these systems is that we can investigate the effects of nonuniformity even in strongly disordered regions[1], whereas it is difficult to experimentally address such regions in solid physics. Disordered systems have been already studied for more than five decades[2], but there are still many open questions. The optical lattices with spatial disorder are expected to give a new insight into these remaining questions, and thus it is an urgent issue to develop the theory for such lattices.

It is another advantage of cold atoms that we can realize the novel systems such as Bose-Fermi mixed systems, multicomponent Fermi systems, and so on. Especially, the recent realization of the quantum degenerate states of atoms with many hyperfine states[3] attracts our attention to multicomponent Fermi systems. Although the multicomponent Fermi systems have also been analyzed for a long period, rich phases and nontrivial properties due to many degrees of freedom are not fully clarified yet. Namely, what kind of state is stabilized as a ground state in multicomponent Fermi systems with spatial nonuniformity is an important one of left issues.

Motivated by these backgrounds, we study N-component Fermi systems with spatial in-homogeneity using a statistical dynamical mean-field theory to address the N=2 case and a Bogoliubov-de Gennes method to the N=3 and 4 cases. The distribution functions of the local density of states and the *s*-wave superfluid order parameter are obtained in N=2. From the geometrical averages estimated from these distribution functions, the ground-state phase diagram of the 2-component Anderson-Hubbard model with the attractive correlation at zero temperature and half-filling is determined. In the N=3 and 4 cases, the charge correlation function, the singlet pairing amplitude, and the free energy of each phase are calculated. In this study, we uncover that spatial disorder induces the phase transition from a density-wave phase to a superfluid phase in 3-component systems. It is also clarified that a further increase of the disorder strength destroys the long-range order of the superfuluid state and thus the superfluid state undergoes a transition to the Anderson localized state. We conclude from the calculations of the free energy of each state that these disorder-driven transitions are of first order. From the similar calculations performed for N=4, it is demonstrated that the density-wave state directly undergoes a transition to the Anderson localized state; there are no regions where the superfluid state is stabilized as a ground-state in 4-component systems. This observation leads us to claim that for N >3 the density-wave state may undergo a direct transition to the Anderson localized state without stabilizing the superfluid state in between. Also, comparing the ground-state phase diagrams of the N=3 and 4 cases determined in this research, we clarify that the density-wave state in N=4 is more robust than that in N=3. This result implies that with an increase of N the density-wave state gradually becomes robust over spatial nonuniformity and possibly other perturbations such as thermal fluctuations.

References

[1] J. Billy *et al.*, Nature **453**, 891-894 (2008).
[2] P. W. Anderson, Phys. Rev. **109**, 1492-1505 (1958).
[3] B. DeMarco *et al.*, Science **285**, 1703-1706 (1999), A. G. Truscott *et al.*, Science **291**, 2570-2572 (2001), T. Fukuhara *et al.*, Phys. Rev. Lett. **98**, 030401 (2007), B. J. DeSalvo *et al.*, Phys. Rev. Lett. **105**, 030402 (2010)

Studies on Non-equilibrium Fluctuating Motion as a Rectifier

Advanced Statistical Dynamics Group Tomohiko Sano

Abstract Fluctuating motion of piston under nonlinear friction is studied as a rectifier of momentum flux. We study the motion of an adiabatic piston under the mechanical equilibrium, which is located between two equilibrium environments characterized by two different temperatures and densities. We show that the direction of momentum flux rectified from the fluctuation piston is not determined by temperature difference, if the piston is attached to non-equilibrium environments.

Extraction of work from systems attached to thermal equilibrium environments is an important topic in thermodynamics and statistical mechanics. The milestone of equilibrium thermodynamics is the Carnot efficiency, which is realized in quasi-static operation and is the maximum efficiency [1]. For practical point of view, the Carnot efficiency is useless, because work per a unit time (power) is zero. Extension of equilibrium thermodynamics toward finite time operation, i.e. finite time thermodynamics, where one can ask the efficiency at maximum power output, has been one of the important topic in non-equilibrium statistical mechanics. Whether the operation is finite time manner or not, we partition the system (gas) in the container by a piston, when we discuss the efficiency or power of the engine. We usually assume that the piston is attached to thermal gases only, and is operated in completely deterministic manner, although the piston itself can be far from thermal equilibrium. Therefore, it is important to consider the extraction of work, when the piston is attached to non-equilibrium environment, or is subjected to non-equilibrium fluctuation.

One of the ubiquitous non-equilibrium environments is friction, which can be regarded as the zero-temperature environment [2]. For practical point of view, controlling a small fluctuating object under friction is important, such as the application to nano-motors under axial friction. Experiments for macroscopic systems under dry friction reveal that the dry friction has an important role to rectify unbiased fluctuations, i.e., to extract work from an equilibrium environment. Although dry friction plays essential roles in non-equilibrium transport and it is ubiquitous throughout nature from a biological surface to an atomic-scale surface, the energetics for the systems under dry friction has been elusive so far. In this talk, we study energy transfer, such as momentum or heat transfer, for systems with a fluctuating boundary under nonlinear friction. For this purpose, we study the one-dimensional motion of an adiabatic piston under the mechanical equilibrium, which is located between two equilibrium environments characterized by two different temperatures and densities. Lieb suggested that the equilibrium thermodynamics cannot tell us whether the adiabatic piston moves or not [3]. This problem is solved analytically by using the Boltzmann-Lorentz equation and is recently phenomenologically understood through the concept of the momentum transfer deficit due to dissipation (MDD) [4]. However, the motion of the adiabatic piston under sliding friction is little known [5].

In the absence of sliding friction, the direction of the piston motion is known to be determined from the difference of temperature of two gases only. However, if sliding friction exists, we show that the direction of motion depends on the amplitude of the friction, and nonlinearity of the friction, i.e. the direction of momentum flux rectified from the fluctuation piston is not determined by temperature difference, if the piston is attached to non-equilibrium environments.

References

[1] H. Callen, *Thermodynamics and an Introduction to Thermostatistics*, 2nd edition (Wiley, New York, 1985).
[2] B. N. J. Persson, *Sliding Friction* (Springer-Verlag, Berlin, 2000).
[3] E. H. Lieb, Physica A **263**, 491 (1999).
[4] Ch. Gruber and J. Piasecki, Physica A **268**, 412 (1999), A. Fruleux, R. Kawai, and K. Sekimoto, Phys. Rev. Lett. **108**, 160601 (2012).
[5] T. G. Sano and H. Hayakawa, Phys. Rev. E **89**, 032104 (2014).

Transition dynamics from macro- to micro-phase separation in asymmetric lipid bilayers

Dissipative Structure and Biological Physics Shunsuke Shimobayashi

Abstract We reveal transition dynamics from macro- to micro-phase separation in multicomponent asymmetric lipid vesicles exposed to externally added glycolipids. Numerical analysis gives us insights into the mechanism of the novel transitions, which is apparently governed by the local spontaneous curvature induced by the local asymmetric lipid composition.

In general, phase separation in binary liquid mixtures completes by relaxation below the transition temperature. The coarsening dynamics to complete phase separation have been extensively investigated in binary mixture systems of polymeric and/or low molecular weight molecules. In contrast, the reverse dynamics from macro- to micro-phase separation remains poorly understood because no appropriate experiments and models exist for investigating this phenomenon.

Phase separation in reconstituted lipid membranes has become intensively researched, because it might explain the nanosized heterogeneities observed in cell plasma membranes. However, micrometer-sized domains are readily reconstituted in giant unilamellar vesicles (GUVs) formed from lipid mixtures. Eventually, these domains are thought to coalescence into a single domain. However, recently it has been suggested that molecular doping with proteins or head-bulky lipids can modulate the stable morphologies of phase separation, enhancing the stability of micro-phase separation [1]. However, the transition dynamics from macro- to micro-phase separation by added guest molecules is still veiled.

In this talk, we present the direct observations of morphological transitions from macro- to micro-phase separation using micrometer-sized asymmetric lipid vesicles exposed to externally added glycolipids (GM1) (Figure 1(a)-(c)). The transition occurs via stripe morphology as a metastable state. During the transition, monodisperse micro domains emerge through repeated scission events of the stripe domains (Figure 1(c)). Moreover, we numerically confirmed the transitions by the time-dependent Ginzburg-Landau model, which describes phase separation and bending elastic membrane (Figure 1(d)). Numerical results suggest the crucial role of the local spontaneous curvature induced by the local asymmetric lipid composition.

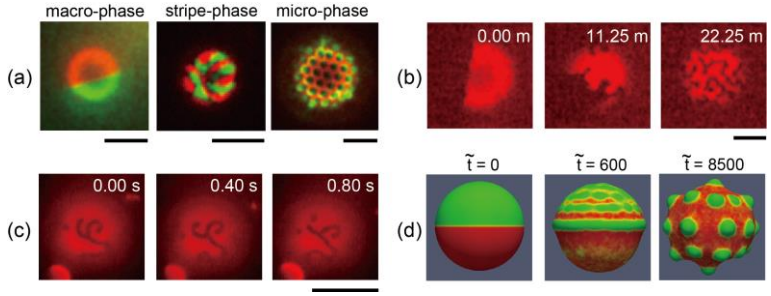

Fig. 1. (a) Top-view images of giant unilamellar vesicles with three distinct morphologies through confocal fluorescent microscopy. (b,c) Sequential top-view images of each vesicle transiting from macro- to stripe-phase and from stripe- to micro-phase, respectively. (d) Transition dynamics from macro- to micro-phase separation in the 3D numerical analysis. Green and red regions represent two different phases, respectively. Scale bars are 5 μm.

References

[1] C. S. Scheve, P. A. Gonzales, N. Momin, and J. Stachowiak, JACS **135** 1185 (2013).
[2] S. F. Shimobayashi, M. Ichikawa, and T. Taniguchi, submitted (arXiv: 1504.03038).

Density-matrix renormalization group study of quantum spin systems with Kitaev-type anisotropic interaction

Physics of Matter: Condensed Matter Physics (YITP)　Kazuya Shinjo

Abstract We study an extended Kitaev-Heisenberg model including anisotropic off-diagonal couplings by using two-dimensional density-matrix renormalization group method. Calculating the ground-state energy and spin-spin correlation functions, we make a phase diagram of the model. The entanglement properties of the Kitaev spin-liquid phase in the phase diagram are discussed.

Since it has been found that the ground state of the Kitaev model on honeycomb lattice provides exactly-solvable examples of spin liquids [1], candidate materials for the model have been investigated. One of the candidates is Na_2IrO_3 in which spin-orbit coupling of Ir plays an important role. Na_2IrO_3 consists of well-separated honeycomb layers, and the Kitaev-Heisenberg model with the Kitaev-type anisotropic exchange interaction coming from strong spin-orbit coupling as well as the usual Heisenberg interaction between Ir ions has been proposed as an effective spin model [2]. However, it has turned out that the model cannot naturally explain zigzag antiferromagnetic order observed in experiments of Na_2IrO_3 [3]. Therefore, further investigation of augmented effective models for Na_2IrO_3 taking into account anisotropic off-diagonal interactions coming from trigonal distortion attracts much attention.

We first consider an extended Kitaev-Heisenberg model including additional anisotropic off-diagonal couplings (model-1) by using two-dimensional density-matrix renormalization group (DMRG) method [4]. Calculating the ground-state energy, the entanglement entropy, and the spin-spin correlation functions, we make the phase diagram of the extended Kitaev-Heisenberg model around the spin-liquid phase. We found a zigzag antiferromagnetic phase, a ferromagnetic phase, a 120-degree antiferromagnetic phase, and two kinds of incommensurate phases around the Kitaev spin-liquid phase. We have checked that the zigzag antiferromagnetic phase is continuously connected to the ground state of a more realistic Kitaev-Heisenberg model (model-2) derived by *ab initio* study of Na_2IrO_3 [5]. Furthermore, we also investigated the model-2 by DMRG and found zigzag antiferromagnetic phases, a 120-degree antiferromagnetic phase, a 16-sites unit cell phase, and an incommensurate phase with changing trigonal distortion.

Finally, we study the entanglement entropy and the entanglement spectrum of the extended Kitaev-Heisenberg model (model-1). These quantities can detect non-local correlation inherent in topologically-ordered states and have recently been introduced to condensed matter physics from quantum informational physics to characterize topological order in fractional quantum Hall states and quantum spin liquids [6]. Then, we found that the entanglement levels in the Kitaev spin-liquid phase are degenerate forming pairs while those in the magnetically ordered phases are non-degenerate. The number of degeneracy depends both on the size of the boundary of the subsystem and on the boundary condition. The Schmidt gap defined by the difference between the two lowest entanglement levels changes at the phase boundaries of the Kitaev spin-liquid phase, although it is not necessarily useful in characterizing phase transitions between magnetically ordered phases.

References

[1] A. Kitaev, Ann. Phys. (NY) **321**, 2 (2006).
[2] J. Chaloupka *et al.*, Phys. Rev. Lett. **105**, 027204 (2010).
[3] S. K. Choi *et al.*, Phys. Rev. Lett. **108**, 127204 (2012); F. Ye, *et al.*, Phys. Rev. B **85**, 180403 (2012).
[4] K. Shinjo *et al.*, Phys. Rev. B **91**, 054401 (2015).
[5] Y. Yamaji *et al.*, Phys. Rev. Lett. **113**, 107201 (2014).
[6] A. Kitaev and J. Preskill, Phys. Rev. Lett. **96**, 110404 (2006); M. Levin and X.-G. Wen, Phys. Rev. Lett. **96**, 110405 (2006).

Estimating effective connectivity between brain areas with DCM

Nonlinear Dynamics Group　Toshiaki Shintani

Abstract Recent advance of fMRI techniques enables us to analyze the connectivity of entire brain. DCM is the estimation method for the connectivity but it is generally difficult to infer a number of connections among many brain areas. We proposed a solution strategy and validated the method.

When our brain processes the external information, the blood flow volume in the regions related with the process changes, and the blood oxygen level changes because of the consumption of oxygen for the activity of neurons. Using this fact, functional magnetic resonance imaging (fMRI) techniques image the brain activity from the change of the blood oxygen level.

The recent advance of fMRI enables the research for the correlation of the brain activity. The networks of the influence of the activity of a brain area over that of another area is called effective connectivity, and the analysis of the connectivity from fMRI data is important for understanding the information processing in the brain. The dynamic causal modeling (DCM) [1] is an estimation method which can analyze the changes in the effective connectivity across the brain areas.

It is well known that fMRI data has many causes of the noise. In the study with DCM, the observation noise is assumed, and it is expected that the original signal fluctuations cannot be detected if the observation noise is large [2]. To examine the manner in which the signals are obscured, we create the data with the connectivity model presented in the previous study [1] and examine the parameter region where one can recover the model from the data for various signal-to-noise ratios (SNRs).

In DCM, we create various connectivity models of the interested brain areas and select the model which can most likely explain the fMRI data. However, the model selection process is difficult to calculate when the number of areas increases. In the present study, we adopted a method of automatically pruning connections based on individual levels of confidence given the data, which does not require arbitrary operations. We estimated with the method for various prior variances of the connections and found the optimal parameter region of the prior variance and the SNRs where one can recover the model.

References

[1] K. J. Friston, L. Harrison, and W. Penny. Dynamic causal modelling. NeuroImage, 19(4):1273–1302, 2003.
[2] T. Shintani and S. Shinomoto. Detection limit for rate fluctuations in inhomogeneous Poisson processes. Phys. Rev. E, 85, 041139, Apr 2012.

Kinetic theory for cohesive granular gases with a square well potential

Advanced Statistical Dynamics Group　Satoshi Takada

Abstract We study the kinetic theory of dilute cohesive granular gases whose attractive part is described by a square well potential. We derive a set of hydrodynamic equations from the kinetic theory with the dissipation rate and the transport coefficients. We also perform the numerical simulations to check the validity of our theory.

Because granular materials are ubiquitous in our daily lives, to understand their properties is important in both physics and industry. Granular materials behave as unusual solids, liquids, and gases. Even though we consider the most idealistic case, a system for a dilute gas without any external force, the system cannot maintain a homogenous state due to inelastic collisions between grains. Such inhomogeneity can be understood by the instability of granular hydrodynamics.

Although the interaction between idealistic granular materials are assumed to be repulsive short range force, cohesive force cannot be ignored for fine powders or wet granular system. In a previous study [1], we have shown the appearance of various phases for cohesive powders under a plane shear. We have also demonstrated that the dynamic van der Waals model under a plane shear can reproduce such phases and clarified the mechanism of the instability which is mainly caused by the cohesive force for small systems [2].

In this study, we extend the kinetic theory of the inelastic hard core system to the nearly elastic granular gases whose attractive part is given by a square well potential. We derive a set of hydrodynamic equations using the Chapman-Enskog theory and obtain the dissipation rate and the transport coefficients of this system [3]. Our theoretical viscosity is consistent with the previous results for elastic gases [4] (Fig. 1). We find that the transport coefficients are identical to those for hard core system of the diameter d (λd) in the high (low) temperature limit (λ is the well width ratio). We also try to examine various numerical methods such as the discrete Monte Carlo simulation and event-driven molecular dynamics simulation to verify the validity of the kinetic theory.

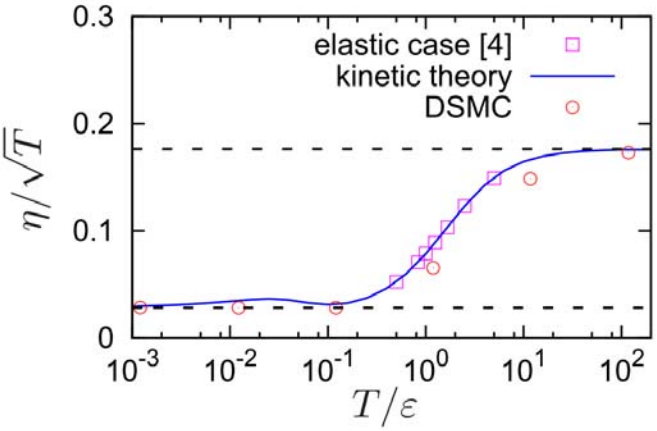

Fig. 1. The granular temperature dependence of the shear viscosity obtained by the kinetic theory and that by the DSMC.

References

[1] S. Takada, K. Saitoh, and H. Hayakawa, Phys. Rev. E **90**, 062207 (2014).
[2] K. Saitoh, S. Takada, and H. Hayakawa, Soft Matter, **11**, 6371 (2015).
[3] S. Takada, K. Saitoh, and H. Hayakawa, arXiv:1506.04578.
[4] E. M. Holleran and H. M. Hulburt, J. Chem. Phys. **19**, 232 (1951).

Ejection-Jet cycle: self-sustaining mechanism of turbulent-laminar interface

Fluid Physics Group Toshiki Teramura

Abstract A self-sustaining interface structure between turbulence and laminar flows is investigated in two-dimensional channel flow. A simple description for the multi-scale interaction between vortex ejections on the both walls (small scale) and a meandering jet (large scale) is introduced.

Sustaining mechanism of nonlinear structures in turbulent flows is one of central issues of recent turbulence studies, which is mainly motivated by "self-sustaining process" (SSP) in minimal plane Couette flow. Different from classical techniques in vortex dynamics, i.e. idealized vortex modeling, these authors used exact, fully-resolved simulations of Navier-Stokes equation without any approximations. We try to extend their techniques to more general flows, e.g. turbulent-laminar interfaces.

We set Reynolds number $Re = 8000 > Re_c$ to make the laminar Poiseuille flow unstable. Then the turbulent region becomes wider by invading the laminar region. We focus on the interface dynamics between turbulent and laminar regions. This interface eventually disappears in a finite computational region since the laminar region turns to turbulence. We utilize filtered simulation technique [1] to keep the interface permanently:

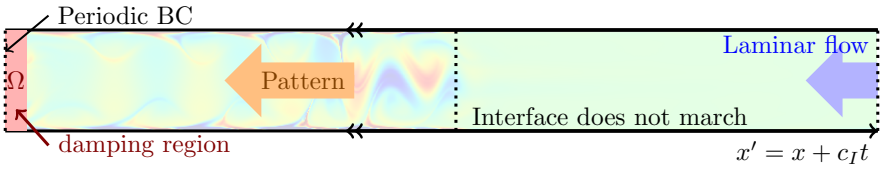

Fig. 1: Setting for the filtered simulation.

$$\frac{\partial \boldsymbol{u}}{\partial t} + (\boldsymbol{u}\cdot\nabla)\,\boldsymbol{u} = -\nabla p + \frac{1}{Re}\nabla^2\boldsymbol{u} - H_\Omega(x')\,(\boldsymbol{u}-\boldsymbol{U}_L), \qquad H_\Omega(x') \approx \begin{cases} 1 & (x'\in\Omega) \\ 0 & (\text{otherwise}), \end{cases}.$$

Since the interface invades at a constant speed c_I, we consider the inertial frame x' where the interface does not march. On this interface frame, we damp turbulence into laminar on a narrow spatial region Ω. This setting approximately corresponds to an infinitely long channel flow setting.

To understand the origin of c_I, we investigate the dynamics of the interface structure. First, we find the interface is self-sustainable; if we damp the turbulent region using the filtered simulation, the interface keeps alive. In addition, the vortex dynamics in the interface is temporally chaotic. So this interface is a self-sustaining coherent structure, and we call it "chaotic interface" (CI). The self-sustaining mechanism of CI is summarized in Fig.2 as "Ejection-Jet cycle", which has two significant properties:

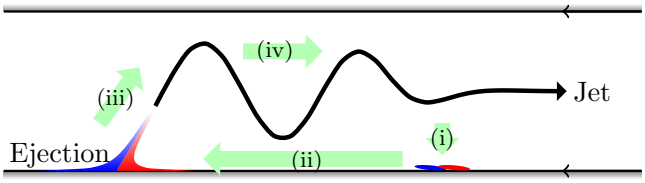

Fig. 2: A schematic figure of Ejection-Jet cycle (quoted from [2]).

- Multi-scale: jet ($\sim 10h$, step (iv)), vortex ejection ($\sim h/500$, step (iii))
- Convective instability (step (ii))

where h denotes the half width of the channel.

References

[1] Toshiki Teramura and Sadayoshi Toh. *Phys.Rev.E*, 89(5):052910, May 2014.
[2] Toshiki Teramura and Sadayoshi Toh. *arXiv (submitted to Phys.Rev.E)* 2015.

Laser spectroscopic study of an atomic Bose-Hubbard system with an atom-number-projection method

Quantum Optics and Laser Spectroscopy Group　Yusuke Nakamura

Abstract By developing a new method of atom-number-projection laser spectroscopy with an ultra-narrow optical transition of ytterbium atoms, we successfully measure a two-particle correlation function from a superfluid to Mott-insulating regime for various temperatures, revealing non-trivial behavior of the temperature and interaction in a finite-temperature phase diagram of a Bose-Hubbard system.

Ultracold atoms in an optical lattice attract considerable attention as a powerful experimental platform to study a strongly-correlated quantum many-body system in a highly controllable way[1]. One can finely control the temperature, the strength of interaction, and atom number with an optical lattice system. Up to now, M. Greiner *et al.*, and S. Trotzky *et al.*, observed a superfluid-Mott insulator (SF-MI) transition[2] and a superfluid-normal fluid (SF-NF) transition[3] experimentally by measuring the matter-wave interference patterns of atomic clouds, respectively. These experiments measure the 1st order correlation function, or a single particle density matrix, which is not sensitive to the behavior of the system other than in a superfluid regime. On the other hand, a spectroscopic method, such as radio-frequency spectroscopy by G. Campbell *et al.* [4] or laser spectroscopy by S. Kato *et al.*, could be utilized for the study not only in SF but also in MI and NF regimes. In fact, S. Kato *et al.* performed laser spectroscopy across a SF-MI transition. However, one needs the careful and sophisticated numerical simulation to extract interesting physics of the system[5].

In this work, by using an ultra-narrow optical transition ($^1S_0$-$^3P_2$) of ytterbium atoms, we established a new laser spectroscopic method of atom-number-projection measurement, in which we suddenly ramp-up an optical lattice potential to quench an atom hopping and thus we can directly measure an atom number distribution in a lattice site as well-resolved spectral peaks. A typical spectrum is shown in Fig. 1. From the measurement, we can deduce the 2nd order correlation function $g^{(2)} = \langle \hat{a}^\dagger \hat{a}^\dagger \hat{a} \hat{a} \rangle$ of an atomic Bose-Hubbard system over SF, MI and NF regimes for various temperatures. Here, $\hat{a}$ and $\hat{a}^\dagger$ represent annihilation and creation operators of an atom, respectively. From the temperature dependence of $g^{(2)}$, we successfully revealed non-trivial behavior of the temperature and interaction in a finite-temperature phase diagram of a Bose-Hubbard system. We will discuss the detail of the result.

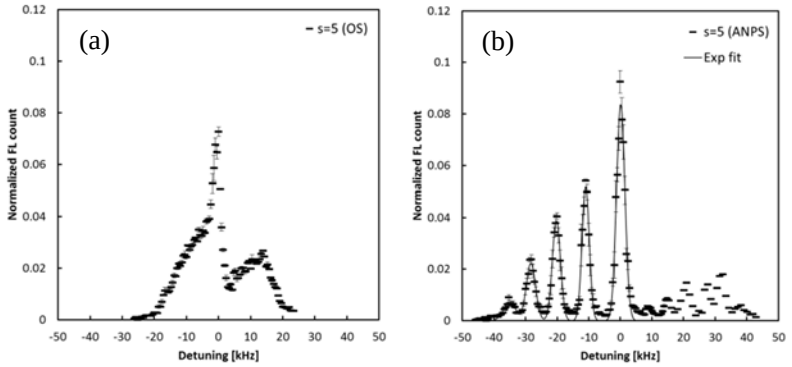

Fig.1 Ordinary spectroscopy (a) and atom-number-projection spectroscopy (b). s is lattice depth.

References

1. I. Bloch *et al*., Rev. Mod. Phys. **80**, 885-964 (2008); D. Jaksch *et al*., Phys. Rev. Lett. **81**, 3108-3111 (1998).
2. M. Greiner *et al*., Nature **415**, 39-44 (2002).
3. S. Trotzky *et al*., Nature **6**, 998-1004 (2010).
4. G. Campbell *et al*., Science **313**, 649-652 (2006).
5. K. Inaba *et al*., arxiv: 1507. 06399v1 (2015).

Dimer solid-liquid transition in the honeycomb compound $Li_{2-x}RuO_3$

Quantum Materials Lab. Marco Polo Jimenez Segura

Abstract: We study the variation of magnetic properties with the crystalline disorder and Li content in $Li_{2-x}RuO_3$ containing Ru honeycomb lattice. We show how the unconventional Ru-dimer liquid-solid transition below $T_d \sim 540$ K depends on the quality of the samples. In addition, we reveal the properties of a new phase with heavily deficient Li content.

Since the discovery of the Ru-Ru dimer transition at $T_d \sim 540$ K in Li_2RuO_3 [1], a number theoretical and experimental groups have been focusing on understanding the precise nature of this dimer transition [2]. Unlike the common Peirls transition proposed initially [3], a recent experiment, using high-energy x rays, suggests that the transition occurs because of the freezing of Ru-Ru dimers from a dimer liquid into dimer solid [2]. Accordingly, a band-structure calculation [2] suggests that at high temperatures the ruthenium spins behave as spin 1/2. Thus, the predictions of phases that exhibit topological superconductivity in honeycomb lattice with the spin $S = 1/2$ [4–6] have impulsed the search for superconductivity at low temperatures.

In the present work, we improved the quality of pristine samples and revealed that the magnetic behavior with the dimmer transition exhibits a strong dependence on the crystallinity and on the cell parameters which vary with the preparation methods [7].

Furthermore, we study the magnetic properties of the de-lithiated "D-phase" $Li_{2-x}RuO_3$. The D-phase is obtained by chemical oxidation of pristine samples using I_2 dissolved in acetonitrile [8]. The change in the crystal structure is found to be congruent with previous studies [8]. Interestingly, we find that the nature of the dimer transition is strongly dependent on the Li content.

Supports from the collaborators are appreciated: S. Kimber at ESRF, France, T. Fröhlic and M. Braden at the Universität zu Köln, Germany, and A. Ikeda, S. Yonezawa and Y. Maeno in the Quantum Materials lab, Kyoto University.

References

[1] Y. Miura, Y. Yasui, M. Sato, N. Igawa, and K. Kakurai, J. Phys. Soc. Jpn. **76**, 033705 (2007).
[2] S. A. J. Kimber, I. I. Mazin, J. Shen, H. O. Jeschke, S. V. Streltsov, D. N. Argyriou, R. Valentí, and D. I. Khomskii, Phys. Rev. B **89**, 081408 (2014).
[3] Y. Miura, M. Sato, Y. Yamakawa, T. Habaguchi, and Y. Ōno, J. Phys. Soc. Jpn. **78**, 094706 (2009).
[4] Y.-Z. You, I. Kimchi, and A. Vishwanath, Phys. Rev. B **86**, 085145 (2012).
[5] T. Hyart, A. R. Wright, G. Khaliullin, and B. Rosenow, Phys. Rev. B **85**, 140510 (2012).
[6] D. D. Scherer, M. M. Scherer, G. Khaliullin, C. Honerkamp, and B. Rosenow, Phys. Rev. B **90**, 045135 (2014).
[7] Marco-Polo Jimenez-Segura, A. Ikeda, S. Yonezawa, and Y. Maeno, Phys. Rev. B submitted (2015).
[8] H. Kobayashi, R. Kanno, Y. Kawamoto, M. Tabuchi, and O. Nakamura, Solid State Ion. **86-88**, 859 (1996).

The effect of the confinement into nano-micelles on the liquid crystalline order

Soft Matter Physics Group Shinji Bono

Abstract We introduced smectic-A liquid crystals (SmA-LCs) into the core of nano-micelles, and investigated the effect of the confinement on the transition behavior of SmA-LCs. As a result, we found that the correlation length of the smectic layer is suppressed by confinement.

Confinement effects change the physical nature of the soft condensed matter characteristic to intrinsic softness of the order and large fluctuation. In liquid crystals (LCs), the confinement affects both the layer order of smectic-A (SmA)-LCs and the orientational order of nematic (N)-LCs. First, we fabricated N-liquid crystalline nano-micelles (LCNMs) in which N-LCs are confined three-dimensionally into NMs with size of several hundred nanometers, and investigated the N-isotropic phase transition behavior of LCs in NMs [1]. As a result, we found that the phase transition behavior changes from the first order to the second order owing to the confinement effect. Next, we fabricated the SmA-LCNMs. SmA-LCs have the one-dimensional layer order together with two-dimensional fluidity. We investigated the confinement effect on the SmA-N phase transition behavior of SmA-LCNMs by measuring the temperature dependence of the correlation length of the layer order, ξ. For the accurate measurement of weak scattering from the tiny LCNMs, we performed synchrotron X-ray at FSBL03XU of SPring-8.

Fig.1 shows the temperature dependence of ξ in NMs together with that in the bulk state. The dashed and dotted lines indicate fitting curves by the power law, $(T-T_{\mathrm{SmA\text{-}N}})^{-\nu}$, where $T_{\mathrm{SmA\text{-}N}}$ is the SmA-N phase transition temperature, and the critical exponent ν=0.48 is assumed as reported by Ref.[2]. Since the SmA-N phase transition in the bulk state is second order phase transition, ξ continuously diverges toward $T_{\mathrm{SmA\text{-}N}}$ on cooling. In the N phase just above $T_{\mathrm{SmA\text{-}N}}$, ξ in NMs diverges in the same way as the bulk state. On the other hand, ξ is saturated below $T_{\mathrm{SmA\text{-}N}}$ and is always shorter than that of SmA-LCs in the bulk state (~1.0×10^4 Å). In order to clarify the confinement effect on the layer order in SmA-LCNMs, we measured ξ as a function of the diameter of LCNMs, as shown in Fig.2. We controlled the diameter of NMs, 2*R*, by changing the ratio of SmA-LC to surfactant [1]. The gray area below the dotted line indicates that the ξ is shorter than 2*R*. ξ proportionally increases as 2*R* increases, and is always shorter than 2*R*. Thus, it can be concluded that the confinement suppresses ξ below the SmA-N phase transition, though confinement does not affect the development of the layer order in the N phase under the condition that ξ is shorter than the diameter of NMs.

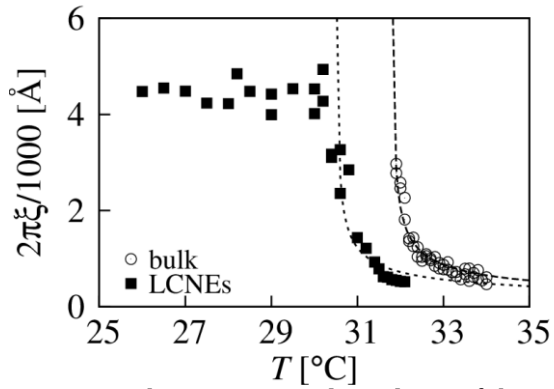

Fig.1 The temperature dependence of the correlation length of the layer order

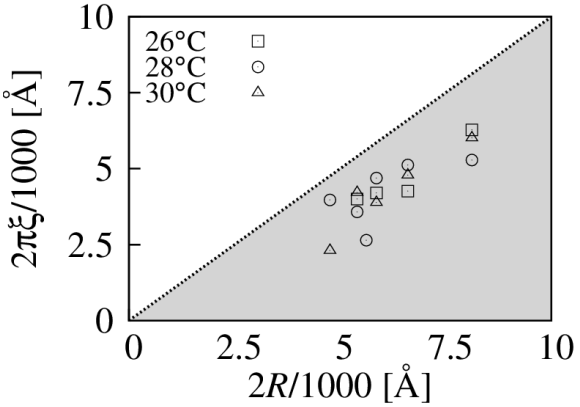

Fig.2 The layer order correlation length as a function of the diameter of the LCNMs.

References

[1] S. Bono, *et al*., *Europhys. Lett.* **109**, 26004 (2015)
[2] Y. Kimoto, *et al*., *J. Phys. Chem. B*, **20**, 6290 (2013)

Nuclear Magnetic Resonance Studies on Heavy Fermion Superlattices

Quantum Materials Lab. Takayoshi YAMANAKA

Abstract We investigated superlattice systems consisting of heavy-fermion (HF) compounds and conventional metals with nuclear magnetic resonance (NMR) microscopically. We succeeded in observing NMR signals of each block layer (BL) and found that the interfaces between the HF and conventional-metal BLs play an important role in the superlattice.

Heavy-fermion (HF) compounds are characterized by the strongly enhanced effective mass of itinerant electrons due to the hybridization between localized *f*-electron and conduction bands at low temperatures. As a result of the duality between itinerant and localized characters of *f*-electrons, various fascinating phenomena have been discovered. Recently, the technique of fabricating epitaxial superlattices consisting of HF compounds and conventional metals has been developed and provides us a new research field on *f*-electron systems [1,2]. For example, in the superlattices consisting of HF superconductor $CeCoIn_5$ and conventional metal $YbCoIn_5$, the value of H_{c2}/T_c is much larger than that of bulk $CeCoIn_5$, where H_{c2} is the superconducting upper critical field at $T = 0$ K and T_c is the critical temperature at $\mu_0 H = 0$ T. In these superlattices, the superlattice structure characterized by the heterostructure (Fig. 1) would play a key role, but the magnetic and electronic properties in each block layer (BL) have not been explored at the microscopic level.

To investigate the magnetic and electronic properties in each BL of the superlattices, we have performed nuclear magnetic resonance (NMR) measurement, which is one of the most suitable microscopic probes, on the $CeCoIn_5(n)/YbCoIn_5(5)$ superlattices as well as the thin films of $CeCoIn_5$ and $YbCoIn_5$, where n (= 5 or 9) layers of $CeCoIn_5$ and 5 layers fixed of $YbCoIn_5$. By comparing the NMR spectra of these samples, we succeeded in identifying the ^{115}In-NMR signals arising from the $CeCoIn_5$ (Ce-) and $YbCoIn_5$ (Yb-) BLs in the superlattices, separately. From the measurements of nuclear spin-lattice relaxation rate ($1/T_1$) in each BL, we found that $1/T_1$ of Ce-BLs is systematically suppressed with decreasing thickness of Ce-BL, although $1/T_1$ of Yb-BLs is essentially unchanged with $1/T_1$ of the $YbCoIn_5$ thin film. The unchanged $1/T_1$ of the Yb-BLs suggests that each BL is nearly isolated and the proximity of *f*-electrons with magnetic moments to the nonmagnetic Yb-BL is unlikely to be the origin of the reduction of $1/T_1$ of Ce-BLs. In addition, we compared the NMR spectra obtained in the superlattices with different thickness of the Ce-BLs, and identified ^{115}In-NMR signals arising from the interfaces and the inner layers. From the measurement of $1/T_1$, we found that antiferromagnetic fluctuations are spatially varied along the *c*-axis even in the one Ce-BL and are significantly suppressed at the interface. Taking into account of these results, we point out the importance of the interfaces in these HF superlattices.

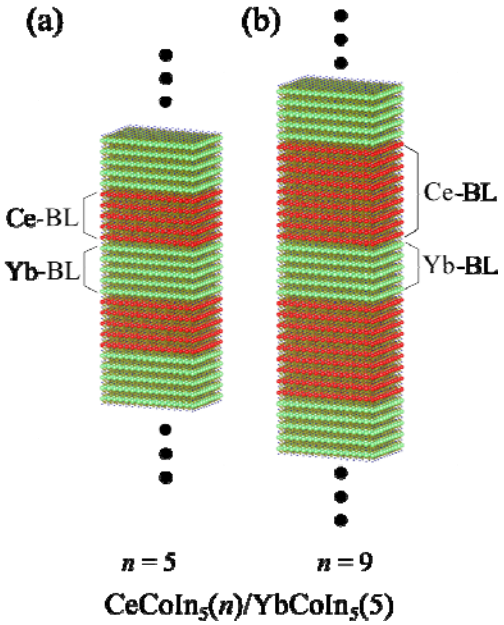

Fig. 1 The schematic image of the superlattices of $CeCoIn_5(n)/YbCoIn_5(5)$. The BLs of n-unit cell thick $CeCoIn_5$ and 5-unit cell thick $YbCoIn_5$ are stacked alternately. The set of Ce-BL and Yb-BL repeats several times.

References

[1] H. Shishido, *et al*., Science **327**, 980-983 (2010).
[2] Y. Mizukami, *et al*., Nature Phys. **7**, 849 (2011).
[3] T. Yamanaka *et al*., submitted for publication.

Study of thermal Hall effect in a frustrated magnet

Laboratory for electronic properties of solids

Daiki Watanabe

Abstract We report that a two-dimensional kagomé insulator volborthite exhibit negative thermal Hall conductivity κ_{xy}. We find that κ_{xy} is absent in the high-temperature paramagnetic state and develops in accordance with the growth of the short-range spin correlations in the spin liquid state. The results suggest the emergence of nontrivial excitations in the spin liquid which acquire fictitious magnetic flux.

When quantum fluctuations suppress the underlying magnetic long-range order, a novel state so called a spin liquid (SL) state often emerges. In such a state the constituent spins are highly correlated but still fluctuate strongly down to much lower temperatures than the spin interaction energy scale, *J*. The low-energy properties in SL systems have been a long-standing mystery. The fluctuations of the spins in a SL have given rise to several notions about novel collective phenomena, such as an emergent gauge field and fractional particle excitations. Several exotic quasiparticles such as spinons and visons have been predicted theoretically. However, the elementary excitations in SL states remain largely unexplored experimentally.

It has been shown that in the insulating quantum magnets, the thermal transport measurements can be used as a probe to unveil the ground state and quasiparticle excitations [1]. Recently, it has been pointed out that the thermal Hall measurements provide new insights into the exotic excitations in magnetic insulators. In magnetic insulators there are no charged currents, and thus the magnetic field cannot exert a Lorentz force. However, the thermal Hall effect has been predicted in disordered magnets as a result of an emergent gauge field [2]. Very recently, it has also been reported in the disordered states but no discernible κ_{xy} signal has been observed in SL states. Thus the thermal Hall conductivity in SL states remains a matter of vital importance.

Volborthite, $Cu_3V_2O_7(OH)_2{\cdot}2H_2O$, is a magnetic insulator, in which 2D layer of Cu^{2+} has a distorted kagomé structure with inequivalent interactions [3, 4]. The temperature dependence of magnetic susceptibility χ shows a typical behavior of 2D frustrated spin system. Below $T^* \sim 60$ K, $\chi(T)$ begins to deviate from the Curie-Weiss behavior, implying that the spin correlations grow gradually when the temperature energy scale k_BT^* becomes comparable to the effective spin interaction energy J_{eff}. Due to the combination of strong geometrical frustration with enhanced quantum fluctuations for $S = 1/2$, the magnetic ordering is suppressed down to $T_N \sim 1$ K (~ 2K) at zero field (15 T), demonstrating the presence of an SL state in a wide temperature range $T_N < T < T^* \sim J_{\mathrm{eff}}/k_B$. χ and C/T extrapolated to $T = 0$ above T_N remains finite, suggesting the gapless spin excitations in the SL state.

Figure 1 depicts the temperature dependence of $-\kappa_{xy}/TB$ at the field of 15 T [5]. Finite thermal Hall signal appears at $T \lesssim T^* \sim 60$ K. The sign of κ_{xy} is negative, i.e. electron-like. As the temperature is lowered, $-\kappa_{xy}/TB$ first develops gradually and then increases steeply below 30 K. After reaching a maximum at around 15 K, $-\kappa_{xy}/TB$ decreases rapidly and changes the sign slightly above T_N. It should be stressed that no discernible thermal Hall signal is observed in the paramagnetic state at $T \gtrsim T^* \sim 60$ K. Moreover, $-\kappa_{xy}/TB$ or $-\kappa_{xy}$ exhibits a peak at around T_p where χ becomes maximum due to the development of the spin-spin correlation length (see the inset of Fig. 1). These results lead us to conclude that the observed thermal Hall effect in volborthite arises from the magnetic excitations in the SL state, not from phonons.

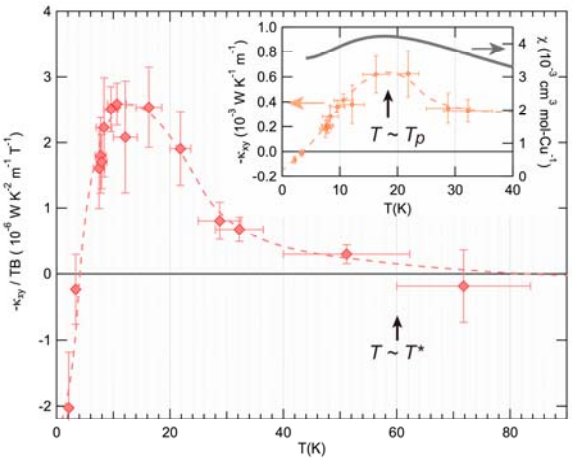

Fig. 1. Temperature dependence of $-\kappa_{xy}/TB$ at 15 T. Inset shows $-\kappa_{xy}$ at 15 T (left) and χ (right). The dotted lines are guides to the eyes.

References

[1] M. Yamashita *et al*., Science **328**, 1246 (2010).
[2] H. Katsura *et. al*., Phys. Rev. Lett. **104**, 066403 (2010).
[3] H. Yoshida *et. al*., Nat. Commun. **3**, 860 (2012).
[4] H. Ishikawa *et. al*.,Phys. Rev. Lett. **114,** 227202 (2015).
[5] D. Watanabe *et. al.*, submitted